

Assessments of Masonry Buildings and Historical Structures during the 2020 Sivrice-Elazığ Earthquake

Alper Özmen^{1*}, Müslüm Murat Maraş¹, Yaşar Ayaz¹, Erkut Sayın²

¹ Department of Civil Engineering, Engineering Faculty, Inonu University, 44000, Malatya, Turkey

² Department of Civil Engineering, Engineering Faculty, Firat University, 23119, Elazığ, Turkey

* Corresponding author, e-mail: alper.ozmen@inonu.edu.tr

Received: 01 November 2022, Accepted: 27 January 2023, Published online: 13 February 2023

Abstract

Turkey is located on a seismically active region. The active fault zones, primarily the North Anatolian Fault and East Anatolian Fault, constitute a center to the movements. On 24 January 2020 at local time 20:55, an earthquake of $M_w = 6.8$ struck Sivrice, Elazığ located in eastern part of Turkey. After this main shock, 1185 aftershocks were recorded until February 8, 2020. The main event resulted in 41 human casualties and 1632 injured. Also, 45 people were salvaged from the debris. The earthquake mostly affected to Elazığ and Malatya provinces. 633 buildings were demolished, 10492 buildings were severely damaged, 2161 buildings were moderately damaged, and 16046 buildings were slightly damaged in the affected region. This paper focus on evaluating the damages and failures of masonry, adobe, and historical structures in the affected areas around Elazığ and Malatya provinces.

Keywords

2020 Sivrice earthquake, seismic performance, masonry buildings, structural damages, field investigation

1 Introduction

Turkey is located in the zone of convergence between the Arabian, African and the Eurasian plates. The westward motion of the Anatolian plate is accommodated by the North and East Anatolian faults [1]. The North and East Anatolian faults connect at Karlıova in the Eastern Anatolia, and they make the Karlıova triple junction. The North Anatolian Fault (NAF) is an almost East-West (E-W) trending right-lateral strike-slip fault for a length of about 1200 km. The NAF forms the transform boundary between the Eurasia and Anatolian plates [2]. The NAF represents the most seismically active fault in Turkey by hosting more than 10 devastating earthquakes in the past 100 years. The East Anatolian Fault (EAF) is an NW-SE trending left-lateral strike-slip fault for a length of about 550 km long [3, 4]. A recent study suggests that a strike-slip tectonic has been effective since late Pliocene [5]. A recent study by [3] divides the EAF into three main sections with several subsegments: the main (southern) branch, the northern strand (Sürgü-Misis fault) and the Karasu trough (Fig. 1(b)). The southern (main) strand includes the Karlıova, İlica, Palu, Pütürge, Erkenek, Pazarcık and Amanos segments.

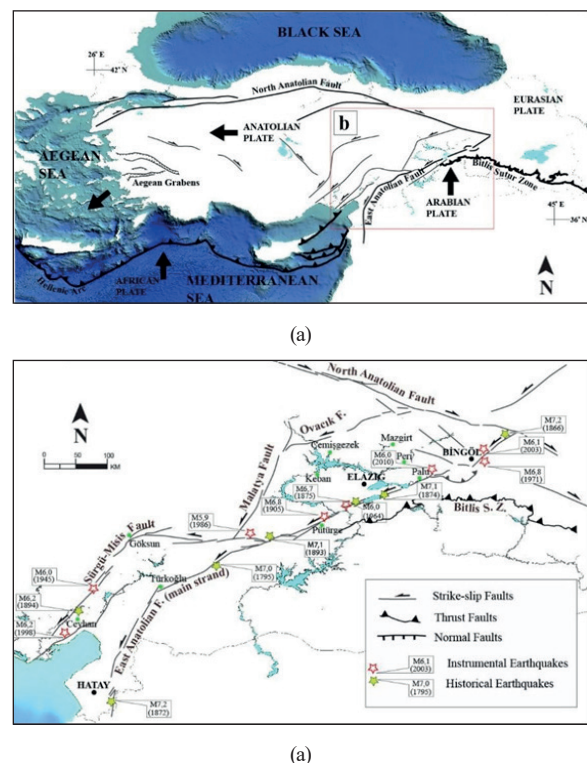


Fig. 1 (a) Simplified main tectonic features of Turkey and westward motion of Anatolian plate (b) Tectonic map of Eastern Anatolia, and historical and instrumental seismicity along the EAF [7]

On Friday, January 24, 2020, a strong earthquake struck Sivrice district of Elazığ at 20:55 (17:55 GMT) local time. This earthquake caused 41 deaths and hundreds of injured people. The earthquake occurred on Pütürge segment on the EAF, which is the most prominent fault in the area (Fig. 1). Many large earthquakes occurred on the EAF in the historical and instrumental periods [3–5]. 8 March 2010 $M_w = 6.1$ at Okçular (Elazığ), 1 May 2003 $M_w = 6.4$ at Bingöl, 27 June 1998 $M_w = 6.2$ at Adana and 5 May 1986 $M_w = 6.0$ at Malatya earthquakes are damaging earthquakes occurred on the EAF in the last century. The historical earthquake catalog summarized by Soysal et al. [6] includes several major earthquakes with uncertain magnitude but with estimated maximum Mercalli intensities as follows: 995 Palu-Elazığ (VI), 1114 Ceyhan-Antakya, (IX), 1268 Kozan-Ceyhan (IX), 1737 Antakya (VII), 1855 Ceyhan-Adana (VI), 1872 Samandağ-Antakya (IX), 1874 Maden-Elazığ, (VIII), 1875 Sivrice-Elazığ (VIII) [6].

After the Sivrice earthquake, based on on-ground field studies: (1) primary surface rupture was not produced by Sivrice earthquake; (2) the Sivrice earthquake produced about 30 landslides; (3) the Sivrice earthquake triggered extensive lateral spreading in Holocene age riverbanks [7]. Turkish Prime Ministry-Disaster and Emergency Management Presidency (DEMA) announced the magnitude of the Elazığ-Sivrice earthquake as $M_w = 6.8$. Also, the coordinates of epicenter were 38.3593 N and 39.0630 E with a focal depth 8.06 km. The effective duration of the earthquake was reported as 20.4 s.

The epicenter was approximately 37 km to the south of the Elazığ city center and 64 km to the east of the Malatya city center [8]. Various institutions explained the magnitude and source characteristics of the earthquake as given in Table 1.

The peak value of ground acceleration was obtained as 0.294 g at the Elazığ-Sivrice station (g is the gravitational acceleration). This value is smaller than the design acceleration value given in Turkish Seismic Code [9] (0.3–0.4 g) and Turkish Building Earthquake Code [10] (0.6–0.7 g).

Table 1 Characteristics of 24.01.2020 Sivrice-Elazığ earthquake

Data Source	Time (GMT)	Latitude (N)	Longitude (E)	hypo (km)	Magnitude (Mw)
AFAD ^a	17:55:11	38.3593	39.0630	8.06	6.8
KOERI ^b	17:55:14	38.3775	39.1042	4.8	6.5
USGS ^c	17:55:14	38.390	39.081	11.9	6.7
EMSC ^d	17:55:14	38.37	39.22	15	6.8

a) Turkish Prime Ministry-Disaster and Emergency Management Agency, DEMA; b) Kandilli Observatory and Earthquake Research Institute; c) United States Geological Survey; d) European-Mediterranean Seismological Centre

Table 2 shows the characteristics of the strong motion accelerations of Sivrice-Elazığ earthquake. In this table, PGA is the peak ground acceleration and R_{epi} is the epicentral distance from the station. The maximum acceleration records of the Sivrice earthquake obtained at Sivrice Station which located approximately 23.8 km to the epicenter. The peak acceleration values of this record are 235.8, 292.8, and 178.6 cm/s^2 for North–South (N-S), East–West (E-W), and Vertical (U-D) components, respectively (Fig. 2).

The earthquake was felt over a very large area including 20 towns in Turkey. It was determined that 633 buildings collapsed, 10492 buildings were severely damaged, 2161 buildings were moderately damaged, and 16046 buildings were slightly damaged in Elazığ and Malatya provinces. After the earthquake, the predicted intensity map prepared automatically shows that the intensity value in the center of the earthquake is $I_0 = VII$ (Fig. 3) [11].

After the mainshock until February 8, 2020, 34 earthquakes between the magnitude 4.0 and 4.9, one earthquake with a magnitude of 5.1 occurred according to the Kandilli Observatory and Earthquake Research Institute (KOERI) (Fig. 4). 1185 aftershocks occurred in the first 16 days (Fig. 5). According to the seismic zone map of Turkey (made by ministry of Public Works and Settlement in 1996 (see DEMA [8] and Fig. 6), Turkey is divided into the five seismic zones. Elazığ is located on the zone 1 and 2 (first- and second-degree earthquake zones). Zone 1 (red-color) represents the highest seismic hazard whereas zone 5

Table 2 Characteristics of the strong motion records of $M_w = 6.8$ Sivrice-Elazığ Earthquake at nearest stations

Station information Name	Latitude (N)	Longitude (E)	R_{epi} (km)	PGA (cm/s^2)		
				N-S	E-W	U-D
2308-Elazığ-Sivrice	38.45	39.31	23.81	235.790	292.803	178.577
4404-Malatya-Pütürge	38.20	38.87	24.55	193.600	228.446	110.623
2301-Elazığ-Merkez	38.67	39.19	36.39	118.144	137.780	65.894
0204-Adıyaman- Gerger	38.03	39.03	36.81	94.312	110.116	59.203
4401-Malatya-Merkez	38.35	38.34	63.04	73.233	87.631	37.353

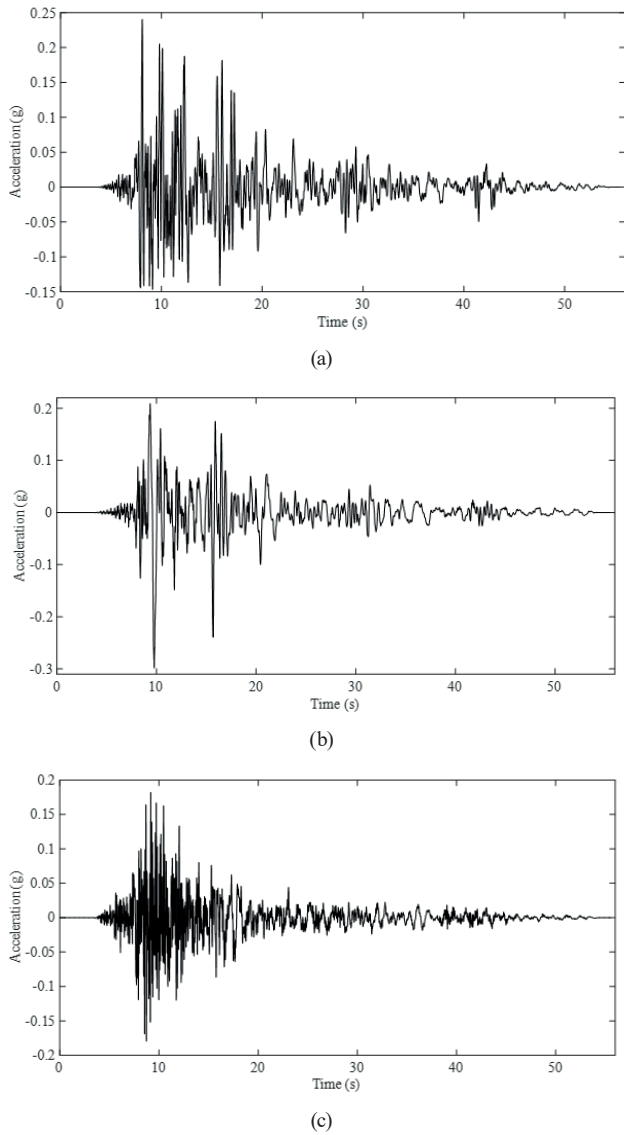


Fig. 2 January 24, 2020 Sivrice-(Elazığ) earthquake acceleration records obtained from the Elazığ-Sivrice station; a) N-S component, b) E-W component, c) U-D component

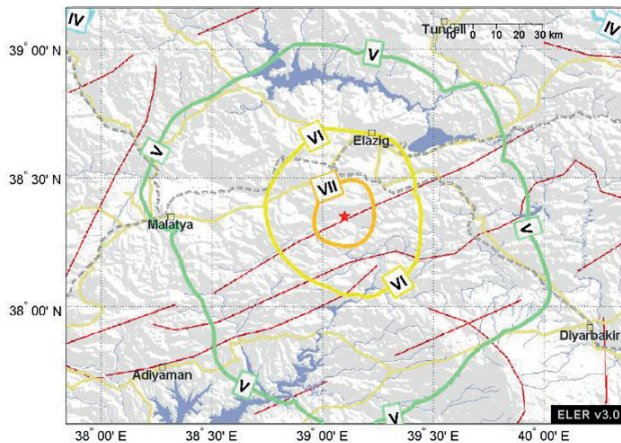


Fig. 3 Intensity map of Elazığ-Sivrice earthquake on 24 Jan 2020 [11]

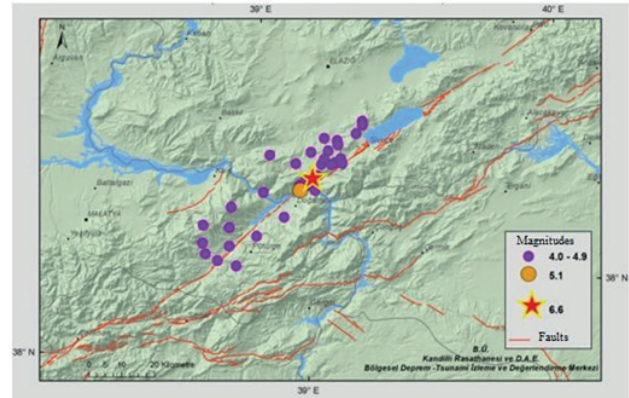


Fig. 4 Sivrice-Elazığ earthquake and aftershocks ($4.0 \leq M \leq 5.1$) until 8 February 2020 [11]

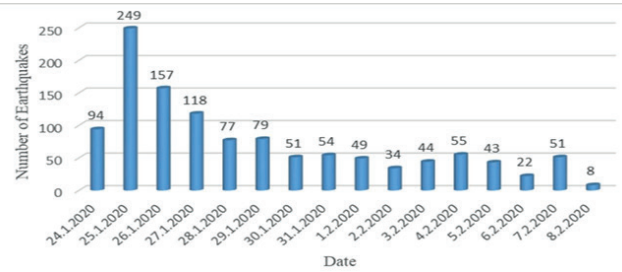


Fig. 5 Numbers of aftershocks until 8 February 2020

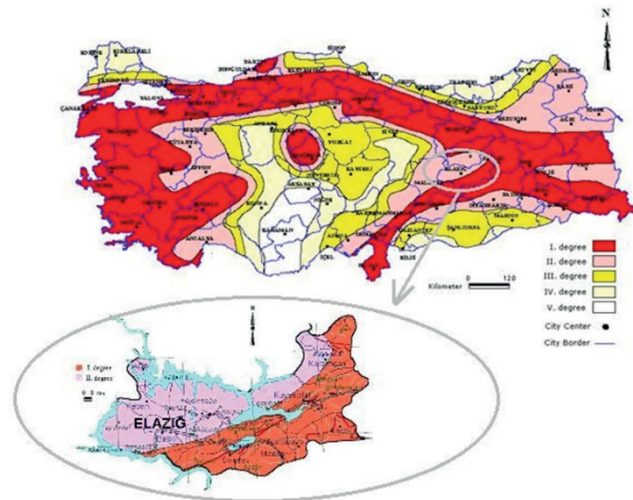


Fig. 6 Seismic zone map of Turkey [8]

(white color) represents no seismic hazard zone. In this map, the first- and second-degree zones require a peak ground acceleration of 0.4 g and 0.3 g for buildings, respectively.

The new earthquake hazard map of Turkey came into force simultaneously with the TBEC- 2018 (Fig. 7). In the new map, earthquake zone concept was removed, and the highest ground acceleration values were described. According to this map, the peak ground acceleration (PGA) values obtained from the 475-year period of the Sivrice-Pütürge segment are 0.6–0.7 g.

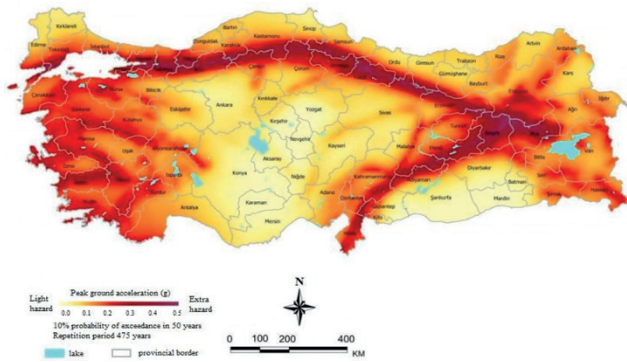


Fig. 7 New earthquake hazard map of Turkey [8]

Several studies had been done relate to structural damages of buildings (adobe, masonry, and reinforced concrete) and field observations after the past earthquakes in various regions. Naseer et al. [12] carried out a field investigation on the seismic behavior of reinforced concrete and masonry buildings in Northern Pakistan during the 2005 Kashmir Earthquake. Also, they presented an overview about 1937 Quetta building code and the 1986 and 2007 building codes of Pakistan. Ural et al. [13] evaluated the seismic response of masonry buildings after the Bala earthquake in 2007. Taucer et al. [14] focused on the seismic response of non-engineered structures (i.e., adobe buildings) during the 2007 Peru earthquake. Zhao et al. [15] investigated building performance during and after the 2008 Wenchuan earthquake in China. They evaluated reinforced concrete frame, reinforced concrete confined masonry, unreinforced and unconfined masonry, industrial, local vernacular, and historical buildings. Augenti and Parisi [16] carried out a study about construction failures of L'Aquila earthquake in Italy. They evaluated significant observed damages with theoretical failure modes for both reinforced concrete and unreinforced masonry buildings. Adanur [17] assessed the seismic performance of unreinforced structures in particularly masonry structures during the 20 and 27 December 2007 Bala-Ankara earthquakes. Celep et al. [18] carried out studies about structural damages of reinforced concrete and masonry buildings after the 2010 Kovancilar and Palu (Elazığ) earthquakes in Turkey.

Kam and Pampanin [19] evaluated the performance of reinforced concrete buildings after the February 22, 2011 Christchurch earthquake in New Zealand. Sorrentino et al. [20] assessed the vernacular buildings which showed very poor seismic performance in the 2012 Emilia earthquakes in Italy. Penna et al. [21] investigated the seismic performance of modern masonry buildings in comparison

to older ones in 2012 in Emilia (Italy) earthquake. Calayır et al. [22] assessed the damages of various structures (reinforced concrete, masonry, adobe and hımiş) during the March 8, 2010 Elazığ-Kovancilar earthquake in Turkey. Ates et al. [23] and Bayraktar et al. [24] carried out a field investigation and investigated the damages of reinforced concrete structures during the 2011 Van earthquakes. Sayın et al. [25] assessed the cause of damages and failures of adobe and masonry structures during the 2011 Maden-Elazığ ($M_w = 5.4$) earthquake in the rural area. Also, they suggested some proposals to improve the earthquake performance of vernacular buildings. The largest of the damages to adobe buildings occurred at the archaeological site of Bam, Iran due to the 2003 Bam earthquake [26]. Indirli et al. [27] analyzed the technical features of unreinforced masonry (URM) buildings and investigated the seismic behavior of these buildings after the Abruzzo 2009 earthquake in Italy. Piroglu and Ozakgul [28] carried out a site investigation about masonry buildings after the 2011 Van earthquakes in Turkey. Sharma et al. [29] assessed field investigation on the performance of building structures during the 2015 Gorkha earthquake in Nepal. They discussed case histories of damaged buildings, the patterns, and the failure mechanisms. Ahmadizadeh and Shakib [30] discussed and evaluated the structural behavior of buildings and lifeline systems in Bam region after 2003 Bam earthquake. Also, some recommendations were given in order to prevent the occurrence of such damages. Atmaca et al. [31] investigated the performance of minarets and mosques in the two affected areas around Elazığ and Malatya provinces after the 2020 Elazığ-Sivrice earthquake. Göçer [32] carried out a study about structural evaluation of masonry buildings in the Tepeköy settlement connected to Gökçeada after the April 24, 2014 Gökçeada earthquake in the Aegean Sea. For this purpose, thirty rural houses which built in the 1960's with traditional materials were evaluated. Temür et al. [33] evaluated geotechnical and structural damages during the 2020 Elazığ-Sivrice earthquake in Turkey. Also, they suggested some suggestions for the preparation of the region in question on active faults for possible earthquakes.

Nemutlu et al. [34] assessed reinforced buildings during the 2020 Elazığ earthquake. Günaydin et al. [35] provides an evolution of seismological characteristics of the earthquake, including recorded accelerograms and acceleration response spectra after the 2020 Elazığ-Sivrice earthquake. Also, the damage and collapse mechanisms observed in masonry building in the earthquake area were

investigated. Sisti et al. [36] investigated the response of buildings in Campi Alto which was strengthened in the past 30 years after the 2016 Central Italy seismic sequence. According to the visual inspections carried out after the 2016 seismic sequence, they obtained that the behavior of buildings in Campi Alto was not satisfactory. Tarque and Panca-Calsin [37] conducted a survey for investigate the construction defects and typologies of house type structures in San Miguel. Additionally, 24 piles and 24 small structural walls were constructed and tested for characterize and examine the physical-mechanical properties of the masonry walls in San Miguel.

In the present paper, the damages and failures of masonry, adobe and historical structures were assessed in the affected areas.

2 Evaluation of structural damages

2.1 Adobe and masonry buildings

In the rural areas, many people still live in adobe and masonry buildings in the various parts of the world. Adobe is one of the oldest building materials. It has been used as a construction material for hundreds of years. This type of construction is used mainly low-income rural populations. Adobe bricks are produced from mixing clay, sand, straw, and water. These mixtures are shaped into bricks and left to dry under the sun. Adobe is very weak against water and mechanical affects. Horizontal wooden ties can be used to increase the bearing capacity of adobe walls. In Turkey, adobe has been widely used in Anatolia since prehistoric times [38]. The foundations of adobe buildings are commonly constituted with stones. Due to advantages of local availability of raw materials, simple construction techniques and insulation properties, adobe and masonry buildings are generally preferred in the rural parts of Turkey. In these buildings, wall thickness varies between 300 mm to 700 mm. Also, lime plaster which is approximately 5 cm was used the interior and exterior surfaces of the adobe and masonry walls. In the area affected by the Sivrice-Elazığ earthquake, the majority of the buildings are adobe in the rural area of Malatya and Elazığ towns which is the most effective regions in the earthquake. Most of the adobe buildings in the earthquake area had been damaged. Also, latest earthquakes demonstrated that adobe and masonry buildings are the vulnerable system to earthquake motions [18, 22, 30]. Also, masonry buildings (stone and brick) generally exist in the earthquake area. These buildings can be classified into two different types in terms of using construction material in the earthquake

region. These are stone and brick masonry buildings. Stone, brick, and adobe materials which are used in masonry and adobe structures have high compressive strength according to tension strength. These structures are constructed in small towns and generally designed for vertical loads according to traditional rules without any engineering services [18, 25]. In Turkey and the area affected by the Sivrice-Elazığ earthquake, construction of unreinforced masonry buildings is common and limited amount of confined masonry buildings co-exists. Stone masonry buildings were constructed with rubble stones gathered from surrounding places. Mud mortars were mostly used instead of cement mortar as binder both stone and brick masonry buildings because of economic reasons [18, 24]. Considerable damages occurred in masonry buildings for different reasons such as poor workmanship and inappropriate construction material. Experience shows that masonry buildings, such as adobe buildings, demonstrated low seismic performance in Turkey even at moderate level earthquakes [13, 24, 28]. Seismic vulnerability assessment is generally focused on structures characterized by the existence of rigid diaphragms whose global response is ruled by in-plane mechanisms. The behavior of masonry structures characterized by a flexible diaphragm is controlled by in-plane and out-of-plane failure mechanisms [39]. This type of diaphragm does not adequately increase the lateral stiffness of the structure [40]. In these buildings, load bearing walls straightly transferred vertical loads to the foundations from the roof and the floors. However, these walls are subjected to in- and out-of-plane bending effects and in-plane shear effects under horizontal forces during the earthquake. Tensile strength of the adobe and masonry material can be easily exceeded during an earthquake, and cracks are suddenly occurred, and they collapse many times. Also, heavy walls and roofs of adobe and masonry buildings are attracted large inertia forces during the earthquake. Nevertheless, adobe walls are thicker than clay brick walls. These heavier walls are attracted larger inertia forces during an earthquake [41]. These forces often result in large cracks or collapse at the adobe and masonry buildings.

The extent of damage to an adobe and masonry building subjected to an earthquake is generally depends on the severity of the ground motion, the geometry of the structure (the configuration of the bearing walls, roof, openings etc.), and the condition of the building. In the earthquake region, one- and two-story adobe and masonry buildings are common. These buildings were built according to traditional

rules by masons or homeowners using local materials with non-engineered services. Because of low strength construction material, adobe buildings have mostly thick, massive and load bearing walls. Therefore, these structures are also termed as non-engineered structures. The most significant weakness of adobe and masonry buildings is that they are made of a material that is weak in terms of both tension and shear.

As the earthquake damage observations and subsequent experiments show that, masonry walls fail in three different failure modes (sliding shear failure, diagonal cracking mode and flexural failure) when subjected to in-plane loads (Fig. 8). Additionally, these various types of failures may occur simultaneously. The failure mechanisms depend on the geometry of the wall (height/width ratio) and quality of materials, but also on boundary restraints and loads acting on the wall [42, 43]. Also, masonry walls show a weak response in perpendicular direction during the earthquake. For this reason, out-of-plane mechanism can generally occur.

In-plane mechanism was observed in most of these buildings that are affected by shear cracking in the earthquake area. Figs. 9 and 10 show in-plane wall failure (diagonal cracking) due to the in-plane load. In the area struck by the Elazığ-Sivrice earthquake, most of the masonry buildings did not have sufficient and proper bond beams to enhance the lateral strength of the walls. The stiffness

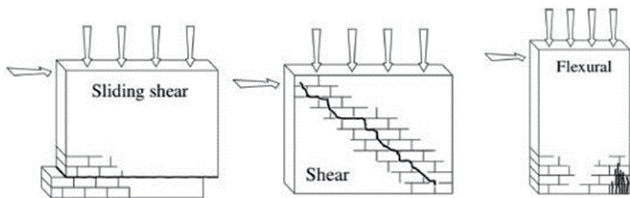


Fig. 8 Typical failure modes of masonry walls, subjected to in-plane seismic load [42]

of the walls has been decreased by large openings on the walls. Also, these openings increased the shear effects. The requirements of the solid walls and openings of load-bearing walls are presented in Fig. 11 [10]. Turkish Seismic Code (TSC) requires the reinforced concrete bond beams to limit this type of failure. Fig. 12 illustrates vertical bond beam which increase the earthquake performance of masonry buildings. Also, Figs. 13(a) and (b) show the horizontal bond beam at the intersection and at the corner of the walls, respectively [9]. A horizontal bond beam above the wall can provide an effective mechanism to transfer the



Fig. 10 Diagonal cracking in masonry buildings



Fig. 9 Diagonal cracking in adobe buildings

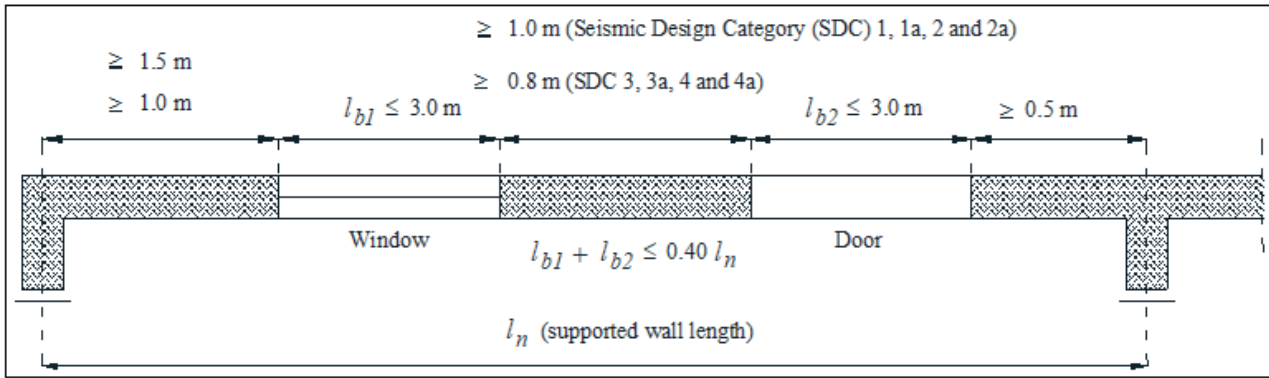


Fig. 11 Some requirements for load-bearing walls according to TBEC, 2018

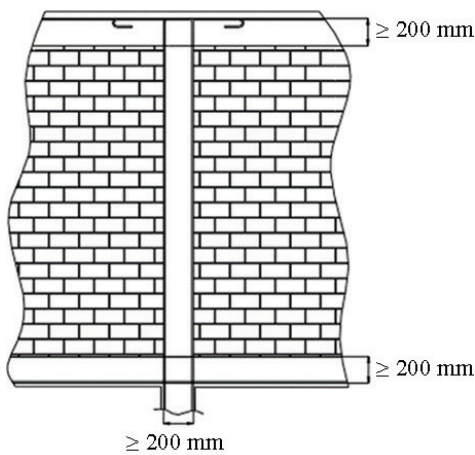


Fig. 12 Vertical bond beam [10]

load between the roof and wall [13]. Load bearing walls are subjected to in-plane and out-of-plane bending effect and in-plane shear effects under lateral earthquake forces. Due to the low shear and flexural strengths, these walls have brittle behavior [28, 33, 44]. Because of the poor connections among the walls and the roofs, lack of horizontal wooden ties, and unsupported wall lengths, each wall

moves individually, and the out-of-plane behavior occurs when subjected to earthquake loads. These wooden ties are used frequently in the stone masonry structures. The out-of-plane performance of unreinforced masonry (URM) walls is weaker than in-plane performance of these walls owing to inherent weakness of masonry in tension. For this reason, even a moderate earthquake causes wall cracking, and the wall undergoes inelastic out-of-plane wall deformations. During earthquakes, load-bearing walls are prone to separation from transverse walls and floors. When there is not adequate continuity in the masonry of orthogonal sets of walls or floors structures are not sufficiently anchored to them, dramatic collapses of both facades and floors are observed [20]. Poor connections among intersecting walls or wall-to-floor connections, using lacking vertical and horizontal bond beams and the length of unsupported walls can cause out-of-plane mechanism. During the earthquake, significant portion or whole of the wall can overturn and cause damage. The separation can occur either vertically or diagonally. Fig. 14 shows some of the common out-of-plane mechanism [45].

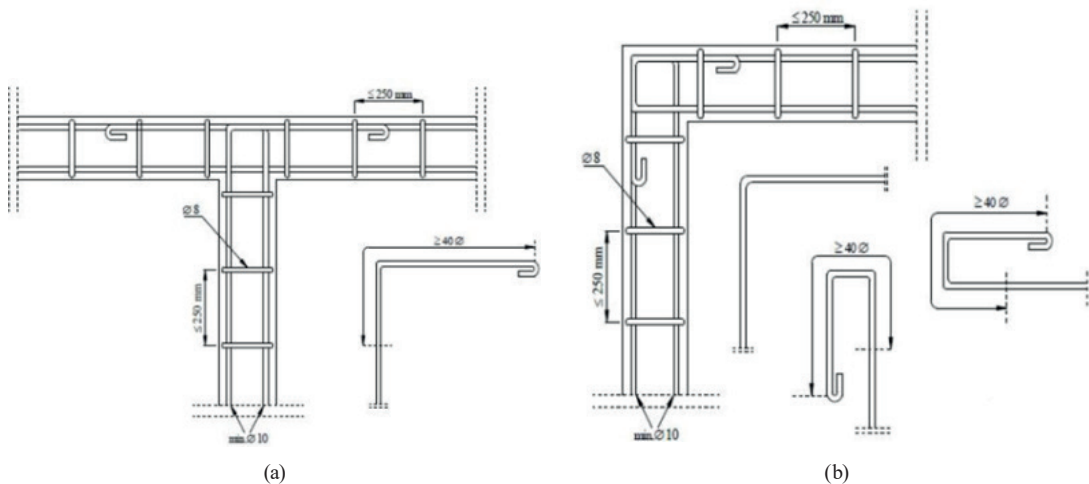


Fig. 13 Details of the horizontal bond beams; (a) intersection of the walls, b) corner of the walls

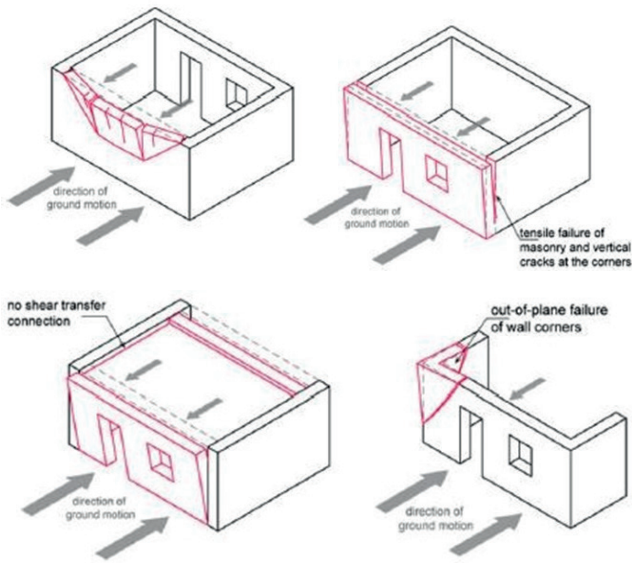


Fig. 14 Damages patterns associated with out-of-plane mechanism [45]

Wooden logs are mostly used as roof beams in Turkey. These logs are placed on two parallel load-bearing walls. Thus, the perpendicular walls which are not restrained at the roof level may easily overturn. Figs. 15 and 16 illustrate out-of-plane movement of the façade wall in an adobe and masonry building, respectively.

Fig. 17 shows overturning of the facades perpendicular to each other. Also, vertical cracks can see in Fig. 17. To prevent these behaviors in masonry buildings, the Seismic Code requires that the maximum unsupported length of a wall should not exceed 5.5 m in the Seismic Design Category (SDC) 1, 1a, 2 and 2a and 7.5 m SDC 3, 3a, 4 and 4a in the plan (Fig. 18(a)). Every 4 m long vertical bond beams should be used in the plan. Also, the unsupported wall length should not exceed 16 m (Fig. 18(b)) [10]. However, most of the masonry structures in the earthquake region did not meet these specifications.



Fig. 15 Out-of-plane wall failure of façade wall in an adobe building



Fig. 16 Out-of-plane wall failure of façade wall in masonry buildings



Fig. 17 Out-of-plane wall failure of façade wall in masonry buildings

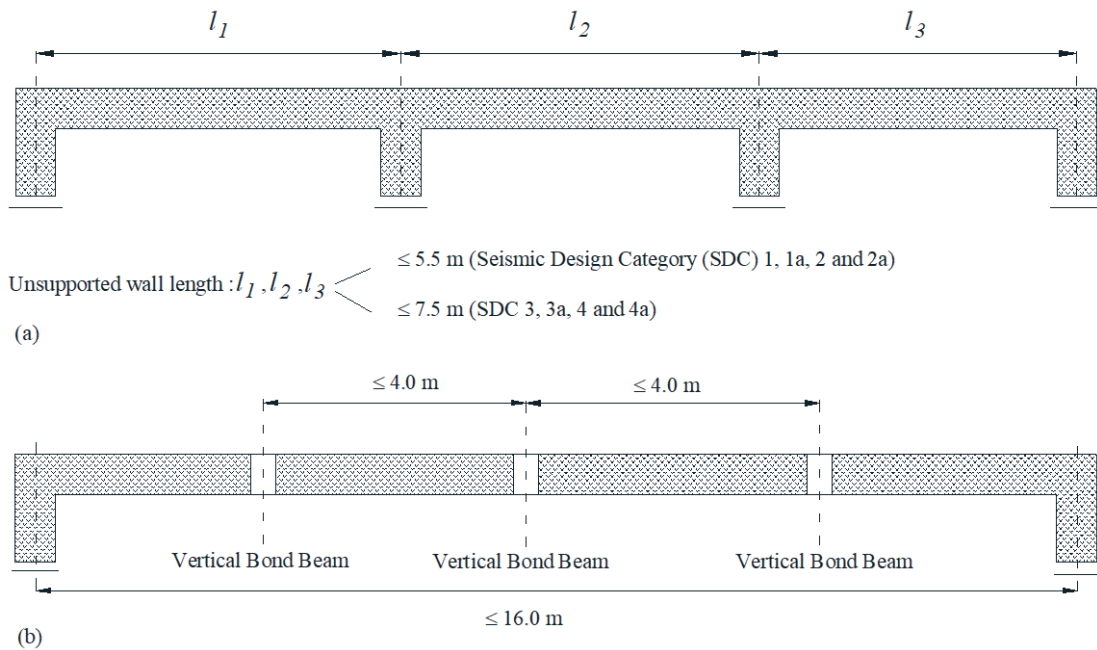


Fig. 18 Maximum unsupported wall length and span between vertical bond beams [10]; a) with reinforced concrete vertical beams, b) without reinforced concrete vertical beams

Also, out-of-plane failure of gable walls were observed in the earthquake region. These components are very vulnerable to out-of-plane lateral loads because they have large unsupported infill walls. They are not well connected to the floor and roof of the structure. Fig. 19 shows the damage of a gable wall.

If the gable walls exceed 2 m in height, Seismic Code requires using vertical and inclined reinforced concrete bond beams to prevent gable wall damages as shown in Fig. 20. Owing to the lack of connection between loadbearing walls and the absence of bond beams, corner damages occur at wall to wall and wall to roof connections when subjected to out-of-plane behavior. Corners connections have high stress concentrations during the earthquake. Due



Fig. 19 Gable wall damages

to cantilever-like behavior, top corners of the buildings are more vulnerable. TSC requires reinforced concrete vertical bond beams to limit corner damage (Fig. 18). These beams increase the seismic performance and lateral stiffness of masonry buildings. Corner damage was a common damage type in the earthquake region. Fig. 21 presents corner damage to masonry and adobe buildings.

Also, disintegration of masonry walls was observed in stone masonry buildings in the earthquake region. Stone masonry buildings which are located on the earthquake area were constructed with multi-leaf walls. Large coarse stones were adopted to arrange the external leaves of the bearing walls, and they covered an internal filling made of with small size stones and mud mortar. Insufficient connections were observed between the exterior and interior layers of the wall. Therefore, layers of these walls behaved independently and separated from each other very easily during the earthquake. Delamination as generally localized in the upper part of the masonry walls. The thickness of these stone walls was approximately 50–60 cm (Fig. 22).

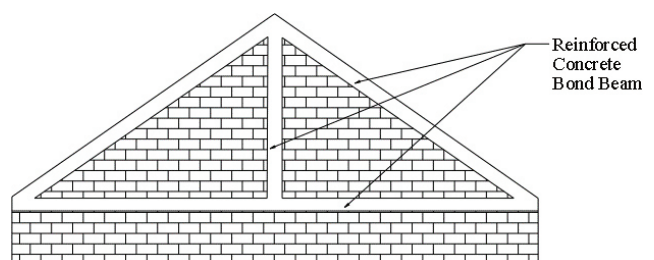


Fig. 20 Reinforced concrete bond beam using gable wall



Fig. 21 Corner damages to adobe and masonry building; a) Adobe building, b) Masonry building

In the earthquake region, heavy earthen roofs were constructed over wooden logs especially in adobe buildings to provide water and thermal insulation. The roofs were generally constituted of dried mud whose thickness ranged between 30 and 100 cm [43, 46]. Because of weather conditions, these roofs lose their effectiveness in winter and the residents made a new earthen layer on top of the existing roof. Therefore, the thickness and weight of the earthen roof increased in time. This type of heavy earthen roofs increased the mass of the buildings and caused large inertial forces during the earthquake motion. Fig. 23 shows the heavy earthen roof and damaged stone masonry building in the earthquake region.

Also, the interior or exterior plaster of adobe and stone masonry walls was partially or totally spalled (Fig. 24). Due to the effects of the strong future aftershocks, these walls can be collapse.

There are also certain masonry buildings built with various materials, such as brick-adobe, stone-brick, and stone-adobe units, which were used either within the same wall



Fig. 22 Disintegration of stone masonry walls (insufficient connection between layers)



Fig. 23 Heavy earthen roof and damaged stone masonry building



Fig. 24 Plaster spalling of the masonry and adobe walls

or different parts of the buildings located in the earthquake region (Fig. 25). Turkish Seismic Code does not allow these type buildings. Different materials caused stiffness and strength concentration in some portions of a wall or in some parts of a building. Under the earthquake loads, this different configuration caused load redistribution problems. Also, additional torsional moments could occur.

2.2 Cultural heritage structures

In the earthquake region, there are some historical structures in Battalgazi town of Malatya (Fig. 26). These cultural heritage structures can be classified as mosques, caravanserais, and mansions. Caravanserais are important and magnificent structures with thick and tall walls. The word caravanserai derives from the Farsi word *kârban* (caravan

and saray (palace). They are nonprofit institutions that have been built on the main roads between cities for accommodation of caravans and passengers. Cultural heritage structures are vulnerable to earthquakes and many external effects (flood, fire, war, wind etc.) and even moderate earthquakes can cause significant damage to these structures [47, 48]. In the region, these heritage structures were constructed with stone, brick, and traditional mortar.

Stones collected from local region were generally used in these structures. The type of stones is based on volcanic tuff. Some of these structures were restored in the past years. Also, volcanic tuff was used for the restoration of these structures. Volcanic stones were obtained from quarry to the west of the Malatya province [49]. Historical mosques can be seen in Fig. 26.



Fig. 25 Masonry buildings having different material; a) Brick and adobe, b) Brick and stone



Fig. 26 Historical structures in Battalgazi town of Malatya

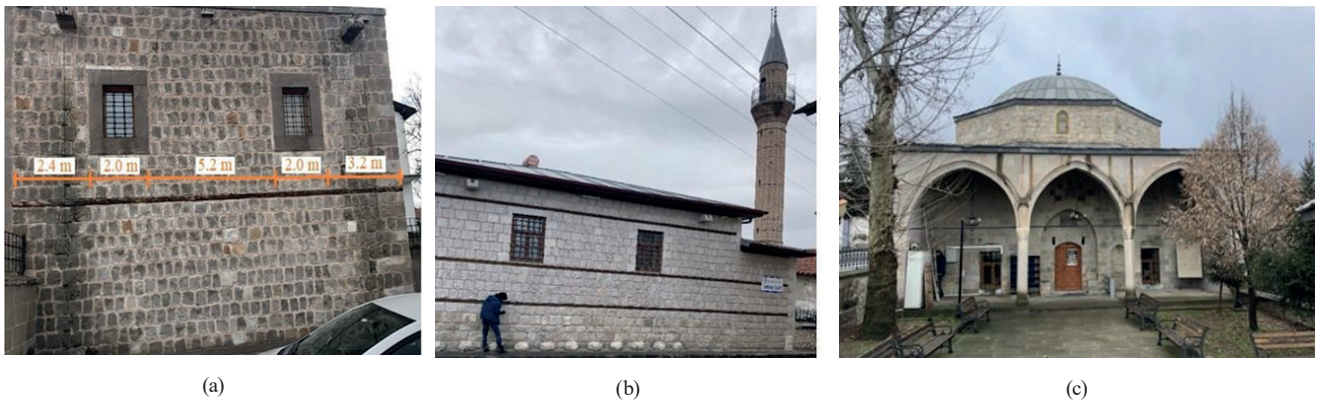


Fig. 27 Undamaged historical structures after the earthquake; a) Karahan mosque, b) Toptaş mosque, c) Akminare mosque

These historical structures had no damage. Karahan and Toptaş mosques are the oldest mosques in the region (Fig. 27(a)–(b)). Karahan and Toptaş mosques were built in 1582 and 1588, respectively. Also, these mosques do not have a dome. Akminare mosque was constructed in 1792 (Fig. 27(c)). Horizontal tie beams were used in these mosques. Openings which increased the shear effects during the earthquake were not close to the corner and each other and these openings were not large.

Also, some thin cracks with limited length were observed at the Silahtar Paşa Caravanserai after the earthquake (Fig. 28). The Silahtar Paşa Caravanserai located in Battalgazi was constructed in 1637 (Fig. 29).

Another historical building is the Yeni Mosque in Malatya. Yeni Mosque was destroyed during the earthquake in 1895. The mosque was rebuilt using cut stones in 1912 with a square plan of 28.5 m. It has five domes, one main dome and four small domes. It was damaged again on June 14, 1964, Adiyaman-Sincik earthquake. The mosque was again repaired after the earthquake. The main dome of the mosque was damaged during the Sivrice-Elazığ earthquake. Some diagonal stepped cracks observed on the wall under the main dome and façade wall of the mosque



Fig. 28 Damage to Silahtar Paşa caravanserai

(Fig. 30). Also, some minor cracks were observed in various parts of the walls. It was closed to worship after the earthquake for repairing (Fig. 31).

3 Conclusions

In this paper, the damages and failures of masonry, adobe and historical structures affected by the 24 January 2020 Sivrice-Elazığ earthquake is presented. In the earthquake, 41 people lost their lives and 1632 injured. Also, extensive seismic damage occurred under such a moderate



Fig. 29 General view of the Silahtar Paşa Caravanserai

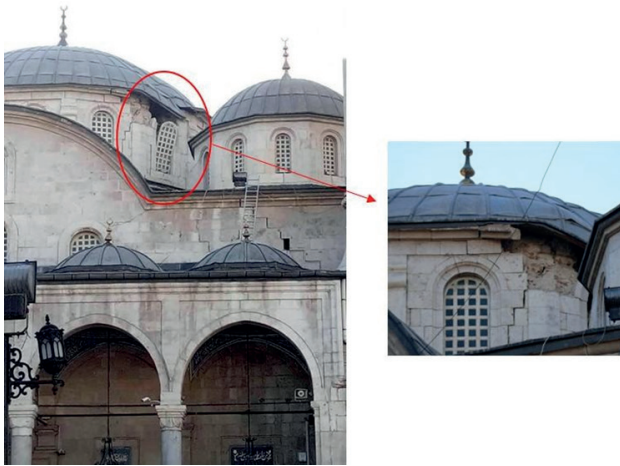


Fig. 30 Damages to Yeni Mosque

earthquake. The achieved value of the peak ground acceleration was 0.294 g. This value is lower than the design acceleration value defined in the Turkish Seismic Code 2007 and 2018. This situation confirmed that the seismic load capacity of unreinforced masonry and adobe buildings is very low. After the earthquake, building construction was started at a total of 67 points in 14 central neighborhoods and 6 districts with an investment cost of 500 million dollars.

After the reconnaissance observations, some of the most common damage causes are given below during the earthquake.

- Multi-story adobe buildings
- Lack and discontinuous of the tie beams
- Heavy earthen roof
- Poor workmanship
- Low strength and quality of the material
- Use of different materials in the same wall
- Multi-leaf walls
- Mud mortar binder
- Insufficient distance between two openings
- High gable walls with non-suitable tie beams
- Out-of-plane failure

References

- [1] McKenzie, D. "Active tectonics of the Mediterranean region", *Geophysical Journal International*, 30(2), pp. 109–185, 1972. <https://doi.org/10.1111/j.1365-246X.1972.tb02351.x>
- [2] Şengör, A. M. C., Tüysüz, O., İmren, C., Sakıncı, M., Eyidoğan, H., Görür, N., Le Pichon, X., Rangin, C. "The North Anatolian fault: A new look", *Annual Review of Earth and Planetary Sciences*, 33, pp. 37–112, 2005. <https://doi.org/10.1146/annurev.earth.32.101802.120415>
- [3] Duman, T. Y., Emre, Ö. "The East Anatolian Fault: geometry, segmentation and jog characteristics", *Geological Society, Special Publications*, 372(1), pp. 495–529, 2013. <https://doi.org/10.1144/SP372.14>
- [4] Köküm, M., İnceöz, M. "Paleostress analysis of the Yeşilyurt-Elazığ Fault Zone and its importance for the tectonic evolution, East Turkey", *Journal of Structural Geology*, 138, 104093, 2020. <https://doi.org/10.1016/j.jsg.2020.104093>
- [5] Köküm, M., Özçelik, F. "An example study on re-evaluation of historical earthquakes: 1789 Palu (Elazığ) earthquake, Eastern Anatolia, Turkey", *Bulletin of the Mineral Research and Exploration*, 161(161), pp. 157–170, 2020. <https://doi.org/10.19111/bulletinofmre.603929>
- [6] Soysal, H., Sipahioğlu, S., Kolçak, D., Altınok, Y. "Historical Earthquake Catalogue of Turkey and Surrounding Area (2100 B.C. – 1900 A.D.)", TÜBİTAK, Ankara, Turkey, Rep. TBAG-341, 1981. (in Turkish)



Fig. 31 General view of the Yeni Mosque after the Sivrice-Elazığ earthquake

In addition, field observations show that the damage ratio increases closer the epicenter and the fault line and resulting in total destruction, especially on the fault line. As a result, the authors can say that if the rural structures are constructed in a way to meet the minimum requirements of seismic codes while benefiting from engineering services, extensive damage will not occur in such a moderate earthquake. In order to prevent such damages of earthquakes in rural areas in the future, the suitability of new buildings should be carefully examined according to the seismic code, and the old buildings that did not receive engineering services should be examined and retrofitted. Design codes should be strict not to allow building construction near fault lines or allow under certain conditions. Also, adobe buildings and earthen roofs built with masonry structures should be prohibited.

Conflict of interest

The authors declare no competing interests.

- [7] Köküm, M. "Landslides and lateral spreading triggered by the 24 January 2020 Sivrice earthquake (East Anatolian Fault)", *Gümüşhane University Journal of Science and Technology*, 11(3), pp. 751–760, 2021.
<https://doi.org/10.17714/gumusfenbil.877544>
- [8] DEMA "Earthquake Department of the Disaster and Emergency Management Presidency", [online] Available: <https://en.afad.gov.tr/>
- [9] TEC "Turkish building earthquake code 2007", [online] Available: <https://turkishtechnic.com/EN/Affiliates/Turkish-Engine-Center>
- [10] TBEC "Turkish building earthquake code 2018", [pdf] Disaster and Emergency Management Agency Ankara, Turkey, 2018. Available: <https://www.resmigazete.gov.tr/eskiler/2018/03/20180318M1-2-1.pdf> (in Turkish)
- [11] KOERI "Boğaziçi University Kandilli Observatory and Earthquake Research Institute Department of Earthquake Engineering", Bogazici University, Istanbul, Turkey, 2020. [online] Available: <http://www.koeri.boun.edu.tr/scripts/lasteq.asp>
- [12] Naseer, A., Khan, A. N., Hussain, Z., Ali, Q. "Observed Seismic Behavior of Buildings in Northern Pakistan during the 2005 Kashmir Earthquake", *Earthquake Spectra*, 26(2), pp. 425–449, 2010.
<https://doi.org/10.1193/1.3383119>
- [13] Ural, A., Doğangün, A., Sezen, H., Angın, Z. "Seismic performance of masonry buildings during the 2007 Bala, Turkey earthquakes", *Natural Hazards*, 60(3), pp. 1013–1026, 2012.
<https://doi.org/10.1007/s11069-011-9887-4>
- [14] Taucer, F., Alarcon, J. E., So, E. "2007 August 15 magnitude 7.9 earthquake near the coast of Central Peru: analysis and field mission report", *Bulletin of Earthquake Engineering*, 7(1), pp. 1–70, 2009.
<https://doi.org/10.1007/s10518-008-9092-3>
- [15] Zhao, B., Taucer, F., Rossetto, T. "Field investigation on the performance of building structures during the 12 May 2008 Wenchuan earthquake in China", *Engineering Structures*, 31(8), pp. 1707–1723, 2009.
<https://doi.org/10.1016/j.engstruct.2009.02.039>
- [16] Augenti, N., Parisi, F. "Learning from construction failures due to the 2009 L'Aquila, Italy, earthquake", *Journal of Performance of Constructed Facilities*, 24(6), pp. 536–555, 2010.
[https://doi.org/10.1061/\(ASCE\)CF.1943-5509.0000122](https://doi.org/10.1061/(ASCE)CF.1943-5509.0000122)
- [17] Adanur, S. "Performance of masonry buildings during the 20 and 27 December 2007 Bala (Ankara) earthquakes in Turkey", *Natural Hazards and Earth System Sciences*, 10(12), pp. 2547–2556, 2010.
<https://doi.org/10.5194/nhess-10-2547-2010>
- [18] Celep, Z., Erken, A., Taskin, B., Ilki, A. "Failures of masonry and concrete buildings during the March 8, 2010 Kovancilar and Palu (Elazig) Earthquakes in Turkey", *Engineering Failure Analysis*, 18(3), pp. 868–889, 2011.
<https://doi.org/10.1016/j.engfailanal.2010.11.001>
- [19] Kam, W. Y., Pampanin, S. "The seismic performance of RC buildings in the 22 February 2011 Christchurch earthquake", *Structural Concrete*, 12(4), pp. 223–233, 2011.
<https://doi.org/10.1002/suco.201100044>
- [20] Sorrentino, L., D'Ayala, D., de Felice, G., Griffith, M. C., Lagomarsino, S., Magenes, G. "Review of out-of-plane seismic assessment techniques applied to existing masonry buildings", *International Journal of Architectural Heritage*, 11(1), pp. 2–21, 2017.
<https://doi.org/10.1080/15583058.2016.1237586>
- [21] Penna, A., Morandi, P., Rota, M., Manzini, C. F., da Porto, F., Magenes, G. "Performance of masonry buildings during the Emilia 2012 earthquake", *Bulletin of Earthquake Engineering*, 12(5), pp. 2255–2273, 2014.
<https://doi.org/10.1007/s10518-013-9496-6>
- [22] Calayır, Y., Sayın, E., Yön, B. "Performance of structures in the rural area during the March 8, 2010 Elazığ-Kovancilar earthquake", *Natural Hazards*, 61(2), pp. 703–717, 2012.
<https://doi.org/10.1007/s11069-011-0056-6>
- [23] Ates, S., Kahya, V., Yurdakul, M., Adanur, S. "Damages on reinforced concrete buildings due to consecutive earthquakes in Van", *Soil Dynamics and Earthquake Engineering*, 53, pp. 109–118, 2013.
<https://doi.org/10.1016/j.soildyn.2013.06.006>
- [24] Bayraktar, A., Altunışık, A. C., Muvafık, M. "Field investigation of the performance of masonry buildings during the October 23 and November 9, 2011, Van Earthquakes in Turkey", *Journal of Performance of Constructed Facilities*, 30(2), 04014209, 2016.
[https://doi.org/10.1061/\(ASCE\)CF.1943-5509.0000383](https://doi.org/10.1061/(ASCE)CF.1943-5509.0000383)
- [25] Sayın, E., Yön, B., Calayır, Y., Karaton, M. "Failures of masonry and adobe buildings during the June 23, 2011 Maden-(Elazığ) earthquake in Turkey", *Engineering Failure Analysis*, 34, pp. 779–791, 2013.
<https://doi.org/10.1016/j.engfailanal.2012.10.016>
- [26] Manafpour, A. R. "Bam earthquake, Iran: Lessons on the seismic behaviour of building structures", presented at 14th World Conference on Earthquake Engineering, Beijing, China, Oct. 12–17, 2008.
- [27] Indirli, M., Kouris, L. A. S., Formisano, A., Borg, R. P., Mazzolani, F. M. "Seismic damage assessment of unreinforced masonry structures after the Abruzzo 2009 earthquake: The case study of the historical centers of L'Aquila and Castelvechio Subequo", *International Journal of Architectural Heritage*, 7(5), pp. 536–578, 2013.
<https://doi.org/10.1080/15583058.2011.654050>
- [28] Piroglu, F., Ozakgul, K. "Site investigation of masonry buildings damaged during the 23 October and 9 November 2011 Van Earthquakes in Turkey", *Natural Hazards and Earth System Sciences*, 13(3), pp. 689–708, 2013.
<https://doi.org/10.5194/nhess-13-689-2013>
- [29] Sharma, K., Deng, L., Noguez, C. C. "Field investigation on the performance of building structures during the April 25, 2015, Gorkha earthquake in Nepal", *Engineering Structures*, 121, pp. 61–74, 2016.
<https://doi.org/10.1016/j.engstruct.2016.04.043>
- [30] Ahmadzadeh, M., Shakib, H. "On the December 26, 2003, south-eastern Iran earthquake in Bam region", *Engineering Structures*, 26(8), pp. 1055–1070, 2004.
<https://doi.org/10.1016/j.engstruct.2004.03.006>
- [31] Atmaca, B., Demir, S., Günaydın, M., Altunışık, A. C. Hüsem, M., Ateş, Ş., Adanur, S., Angın, Z. "Lessons learned from the past earthquakes on building performance in Turkey", *Journal of Structural Engineering & Applied Mechanics*, 3(2), pp. 61–84, 2020.
<https://doi.org/10.31462/jseam.2020.02061084>
- [32] Göçer, C. "Structural evaluation of masonry building damages during the April 24, 2014 Gökçeada earthquake in the Aegean Sea", *Bulletin of Earthquake Engineering*, 18(7), pp. 3459–3483, 2020.
<https://doi.org/10.1007/s10518-020-00833-z>

- [33] Temür, R., Damcı, E., Öncü-Davas, S., Öser, C., Sarğın, S., Şekerci, Ç. "Structural and geotechnical investigations on Sivrice earthquake (Mw = 6.8), January 24, 2020", *Natural Hazards*, 106(1), pp. 401–434, 2021.
<https://doi.org/10.1007/s11069-020-04468-w>
- [34] Nemutlu, O. F., Balun, B., Sari, A. "Damage assessment of buildings after 24 January 2020 Elazığ-Sivrice earthquake", *Earthquakes and Structures*, 20(3), pp. 325–335, 2021.
<https://doi.org/10.12989/eas.2021.20.3.325>
- [35] Günaydin, M., Atmaca, B., Demir, S., Altunişik, A. C., Hüsem, M., Adanur, S., Ateş, S., Angin, Z. "Seismic damage assessment of masonry buildings in Elazığ and Malatya following the 2020 Elazığ-Sivrice earthquake, Turkey", *Bulletin of Earthquake Engineering*, 19(6), pp. 2421–2456, 2021.
<https://doi.org/10.1007/s10518-021-01073-5>
- [36] Sisti, R., di Ludovico, M., Borri, A., Prota, A. "Seismic performance of strengthened masonry structures: actual behaviour of buildings in Norcia and Campi Alto during the 2016 Central Italy seismic sequence", *Bulletin of Earthquake Engineering*, 20(1), pp. 321–348, 2022.
<https://doi.org/10.1007/s10518-021-01248-0>
- [37] Tarque, N., Pancca-Calsin, E. "Building constructions characteristics and mechanical properties of confined masonry walls in San Miguel (Puno-Peru)", *Journal of Building Engineering*, 45, 103540, 2022.
<https://doi.org/10.1016/j.jobe.2021.103540>
- [38] Tanaçan, L. "Adobe construction: a case study in Turkey", *Architectural Science Review*, 51(4), pp. 349–359, 2008.
<https://doi.org/10.3763/asre.2008.5139>
- [39] Sumerente, G., Lovon, H., Tarque, N., Chácará, C. "Assessment of combined in-plane and out-of-plane fragility functions for adobe masonry buildings in the Peruvian Andes", *Frontiers in Built Environment*, 6, 52, 2020.
<https://doi.org/10.3389/fbuil.2020.00052>
- [40] Tarque, N., Crowley, H., Pinho, R., Varum, H. "Displacement-based fragility curves for seismic assessment of adobe buildings in Cusco, Peru", *Earthquake Spectra*, 28(2), pp. 759–794, 2012.
<https://doi.org/10.1193/1.4000001>
- [41] Rafi, M. M., Varum, H. "Seismic performance of adobe construction", *Sustainable and Resilient Infrastructure*, 2(1), pp. 8–21, 2017.
<https://doi.org/10.1080/23789689.2017.1278996>
- [42] Tomazevic, M. "Earthquake-resistant design of masonry buildings", *World Scientific*, 1999. ISBN 978-1-86094-066-8
<https://doi.org/10.1142/p055>
- [43] Sayin, E., Yon, B., Calayir, Y., Gor, M. "Construction failures of masonry and adobe buildings during the 2011 Van earthquakes in Turkey", *Structural Engineering and Mechanics*, 51(3), pp. 503–518, 2014.
<https://doi.org/10.12989/sem.2014.51.3.503>
- [44] Bruneau, M., Yoshimura, K. "Damage to masonry buildings caused by the 1995 Hyogo-ken Nanbu (Kobe, Japan) earthquake", *Canadian Journal of Civil Engineering*, 23(3), pp. 797–807, 1996.
<https://doi.org/10.1139/196-889>
- [45] Ortega, J., Vasconcelos, G., Rodrigues, H., Correia, M., Lourenço, P. B. "Traditional earthquake resistant techniques for vernacular architecture and local seismic cultures: A literature review", *Journal of Cultural Heritage*, 27, pp. 181–196, 2017.
<https://doi.org/10.1016/j.culher.2017.02.015>
- [46] Maras, M. M., Kose, M. M., Rızaoglu, T. "Microstructural characterization and mechanical properties of volcanic tuff (Malatya, Turkey) used as building stone for the restoring cultural heritage", *Periodica Polytechnica Civil Engineering*, 65(1), pp. 309–319, 2021.
<https://doi.org/10.3311/PPci.16977>
- [47] Marra, F., Milana, G., Pecchioli, L., Roselli, P., Cangi, G., Famiani, D., Mercuri, A., Carlucci, G. "Historical faulting as the possible cause of earthquake damages in the ancient Roman port city of Ostia", *Journal of Seismology*, 24(4), pp. 833–851, 2020.
<https://doi.org/10.1007/s10950-019-09844-z>
- [48] Castori, G., Borri, A., De Maria, A., Corradi, M., Sisti, R. "Seismic vulnerability assessment of a monumental masonry building", *Engineering Structures*, 136, pp. 454–465, 2017.
<https://doi.org/10.1016/j.engstruct.2017.01.035>
- [49] Kasap, S., Zengin, B. "Tokat–Restoration of The Caravansaray of Pazar Mahperi Hatun", *The Online Journal of Science and Technology*, 7(3), pp. 150–159, 2017.